



## OPEN ACCESS

## EDITED BY

Thomas Hieronymus,  
University Hospital RWTH Aachen, Germany

## REVIEWED BY

Beatriz León,  
National Institute of Allergy and Infectious  
Diseases (NIH), United States  
Christian H. K. Lehmann,  
University Hospital Erlangen, Germany

## \*CORRESPONDENCE

Botond Z. Igyártó

✉ botond.igyarto@jefferson.edu

RECEIVED 14 April 2025

ACCEPTED 26 June 2025

PUBLISHED 18 July 2025

## CITATION

Bouteau A, Qin Z, Zurawski S, Zurawski G and  
Igyártó BZ (2025) Langerhans cells drive Tfh  
and B cell responses independent of  
canonical cytokine signals.  
*Front. Immunol.* 16:1611812.  
doi: 10.3389/fimmu.2025.1611812

## COPYRIGHT

© 2025 Bouteau, Qin, Zurawski, Zurawski and  
Igyártó. This is an open-access article  
distributed under the terms of the [Creative  
Commons Attribution License \(CC BY\)](#). The  
use, distribution or reproduction in other  
forums is permitted, provided the original  
author(s) and the copyright owner(s) are  
credited and that the original publication in  
this journal is cited, in accordance with  
accepted academic practice. No use,  
distribution or reproduction is permitted  
which does not comply with these terms.

# Langerhans cells drive Tfh and B cell responses independent of canonical cytokine signals

Aurélie Bouteau<sup>1</sup>, Zhen Qin<sup>1</sup>, Sandra Zurawski<sup>2,3</sup>,  
Gerard Zurawski<sup>2,3</sup> and Botond Z. Igyártó<sup>1\*</sup>

<sup>1</sup>Department of Microbiology and Immunology, Thomas Jefferson University, Philadelphia, PA, United States, <sup>2</sup>Baylor Scott and White Research Institute, Dallas, TX, United States, <sup>3</sup>Vaccine Research Institute, INSERM, Unité U955, Institut Mondor de Recherche Biomédicale, Créteil, France

Dendritic cells (DCs) are key regulators of adaptive immunity, guiding T helper (Th) cell differentiation through antigen presentation, co-stimulation, and cytokine production. However, in steady-state conditions, certain DC subsets, such as Langerhans cells (LCs), induce T follicular helper (Tfh) cells and B cell responses without inflammatory stimuli. Using multiple mouse models and *in vitro* systems, we investigated the mechanisms underlying steady-state LC-induced adaptive immune responses. We found that LCs drive germinal center Tfh and B cell differentiation and antibody production independently of interleukin-6 (IL-6), type-I interferons, and ICOS ligand (ICOS-L) signaling, which are critical in inflammatory settings. Instead, these responses relied on CD80/CD86-mediated co-stimulation. Our findings challenge the conventional three-signal paradigm by demonstrating that canonical cytokine signaling is dispensable for LC-mediated Tfh and B cell responses in steady-state. These insights provide a framework for understanding homeostatic immunity and the immune system's role in maintaining tolerance or developing autoimmunity under non-inflammatory conditions.

## KEYWORDS

Langerhans cell, steady - state, adaptive immunity, dendritic cell, TFH, B cell

## Introduction

Dendritic cells (DCs) are critical in training and educating naïve T cells and their differentiation into specific T helper subsets (1, 2). Generally, it is widely accepted that the DCs provide three signals to naïve T cells in the form of cognate peptide/MHC, membrane-bound co-stimulation, and soluble cytokines. Out of these, the cytokines, as third signals (3), are regarded as key components in T helper cell differentiation into T helper subsets, such as Th1, Th2, Th17, Tfh cells, and others (2, 4). These distinct Th subsets are thought to be induced by the DC-derived polarizing cytokines specific for each Th subset. The Th polarizing cytokines are induced by exposure to various inflammatory stimuli sensed by DC through distinct pathogen-associated molecular pattern receptors (5). This oversimplified model of Th differentiation provides a plausible explanation for inflammatory settings, but it

is challenging to apply in a broader sense. For example, antigen targeting to different mouse DC subsets in steady-state in the apparent lack of adjuvant and other inflammatory signals induces Tfh cells and antibody responses (6–15). Furthermore, anti-commensal responses, termed homeostatic immunity, happen regularly in the absence of overt inflammation (16), justifying the need to understand better the induction mechanism of adaptive immune responses in this non-inflammatory context.

Mouse LCs with monocytic origin but DC functions (17–19) drive Tfh cells and germinal center (GC)-dependent protective antibody responses in steady-state (6, 7). They do this irrespective of the nature of the receptor targeted and without signs of activation and maturation (6, 7). Similarly, primary human LCs and CD34<sup>+</sup> cord-blood-derived LCs, unlike monocyte-derived DCs, also support Tfh differentiation and B cell responses *in vitro* without adjuvants upon antigen delivery through Langerin (7, 15). However, the mechanism by which LCs support adaptive immune responses in steady-state remains elusive. Therefore, here, we set out to define the mechanism. We found that LCs induced Tfh and B cell responses independently from IL-6, type-I interferon, and ICOS-L, which were previously reported to play critical roles in inflammatory settings in driving Tfh cells and antibody responses (20–22). LC-induced responses, however, were dependent on CD80/CD86 co-stimulation.

## Results

### LCs, unlike cDC1s, induce GC-Tfh cells and antibody responses in steady-state

We have previously shown using two mouse models that steady-state antigen targeting to LCs, but not cDC1, leads to GC-Tfh formation and antibody responses (7). In mouse skin, Langerin expression is confined to LCs and CD103<sup>+</sup>/XCR-1<sup>+</sup> cDC1s (23), and thus, we used two mouse models, huLangerin and Batf3<sup>-/-</sup> mice, to permit targeting antigen to either LCs or cDC1s. The huLangerin mice express human Langerin specifically in LCs (24), allowing antigen targeting to LCs in the presence of cDC1s using anti-human Langerin (6, 7, 25). The Batf3<sup>-/-</sup> mice lack the migratory Langerin-expressing cDC1s. Therefore, the remaining LCs can be specifically targeted using anti-mouse Langerin (6, 7). To further strengthen our previous findings and increase rigor, here, we expanded our toolset to include two other mouse models specifically affecting cDC1s that were more recently generated by the Murphy lab, IRF8<sup>32Δ</sup>, and XCR1-Cre (26, 27) bred to “STOP”-DTA (Figure 1A; Supplementary Figure S1). The huLangerin-DTA (huL-DTA) mice that lack LCs (28) were used as controls for cDC1s targeting that does not induce GC-Tfh cells and antibody responses in steady-state (6, 7). The indicated mouse strains were adoptively transferred with CD4<sup>+</sup> TEα cells and injected with 1 μg of anti-muLangerin-Eα a day later (Figure 1B). Four and fourteen days later, the antigen-specific CD4<sup>+</sup> TEα T cell and B cell (the targeting constructs have a human IgG4 core that allows measuring the B cell responses mounted) responses were characterized using flow cytometry and ELISA (Figure 1B), as

described previously (6, 7). We found that antigen targeting to LCs in both XCR1-Cre-DTA and IRF8<sup>32Δ</sup> mice, similar to Batf3<sup>-/-</sup> mice, resulted in comparable expansion and differentiation of TEα cells, characterized predominantly by GC-Tfh phenotype (PD-1<sup>+</sup>, CXCR5<sup>+</sup>, Bcl-6<sup>+</sup>) (Figure 1C; Supplementary Figure S1). This contrasts sharply with the outcome of targeting cDC1s in huL-DTA mice, which, in agreement with the previous reports, elicited a distinct T helper response (Figure 1C; Supplementary Figure S1). The B cell responses mounted in these two new models followed a largely similar trajectory to Batf3<sup>-/-</sup> mice but were slightly less pronounced (Figure 1D; Supplementary Figure S1). Interestingly, the IRF8<sup>32Δ</sup> mice did not produce significant levels of antibodies, unlike XCR1-Cre-DTA and Batf3<sup>-/-</sup> mice (Figure 1E). This could indicate that this IRF8<sup>32Δ</sup> deletion might affect GC and plasma cell responses, as has been reported for full IRF8<sup>-/-</sup> mice (29, 30). Thus, these data further support our previous observation that LCs, unlike cDC1s, can induce GC-Tfh cells and antibody responses in steady-state, irrespective of the mouse model used.

### Type I interferon is not required for the induction of adaptive immune responses by steady-state LCs

It is unknown how adaptive immune responses, including Tfh cells and antibody responses, are induced by LCs and some DC subsets in steady-state. Intact type-I interferon signaling in DCs is needed to effectively induce Tfh cells in inflammatory settings through IL-6 up-regulation (31). Targeted delivery of IFNα to cDC1 through Langerin enables these cells to support the differentiation of GC-Tfh cells and GC-dependent antibody responses (7). Based on these data, we hypothesized that steady-state levels of type-I interferon signaling in LCs might play a role in inducing Tfh cells and B cell responses in steady-state. To test this hypothesis, we bred the huLangerinCre mice to IFNαR1<sup>fl/fl</sup> mice to delete IFNαR1 from LCs (Figure 2A). The genotypes of the resulting mice were determined using standard PCR, while the selective deletion of IFNαR1 protein on LCs was confirmed using flow cytometry (Supplementary Figure S2A). Cre-positive and cre-negative mice were then adoptively transferred with CD4<sup>+</sup> TEα cells and, a day later, were injected with 1 μg of anti-huLangerin-Eα. Four and fourteen days later, the antigen-specific CD4<sup>+</sup> T cell and B cell responses were characterized using flow cytometry and ELISA. The anti-huIgG IgG levels were determined using ELISA on serum samples harvested on day 14 (Figure 2A). We found no major differences regarding antigen-specific CD4<sup>+</sup> T cell and B cell expansions and phenotype. The percent of Tfh cells slightly decreased but this was not reflected in the B cell responses. (Figures 2B, C). The anti-huIgG4 IgG levels were also unaffected without type-I interferon signaling in LCs (Figure 2D). These data, therefore, point to the lack of a critical role of type-I interferon signaling in LCs in the steady-state induction of Tfh cells and antibody responses.

To increase the rigor of our findings, we used a blocking antibody against IFNαR (Figure 2E; Supplementary Figure S2B),

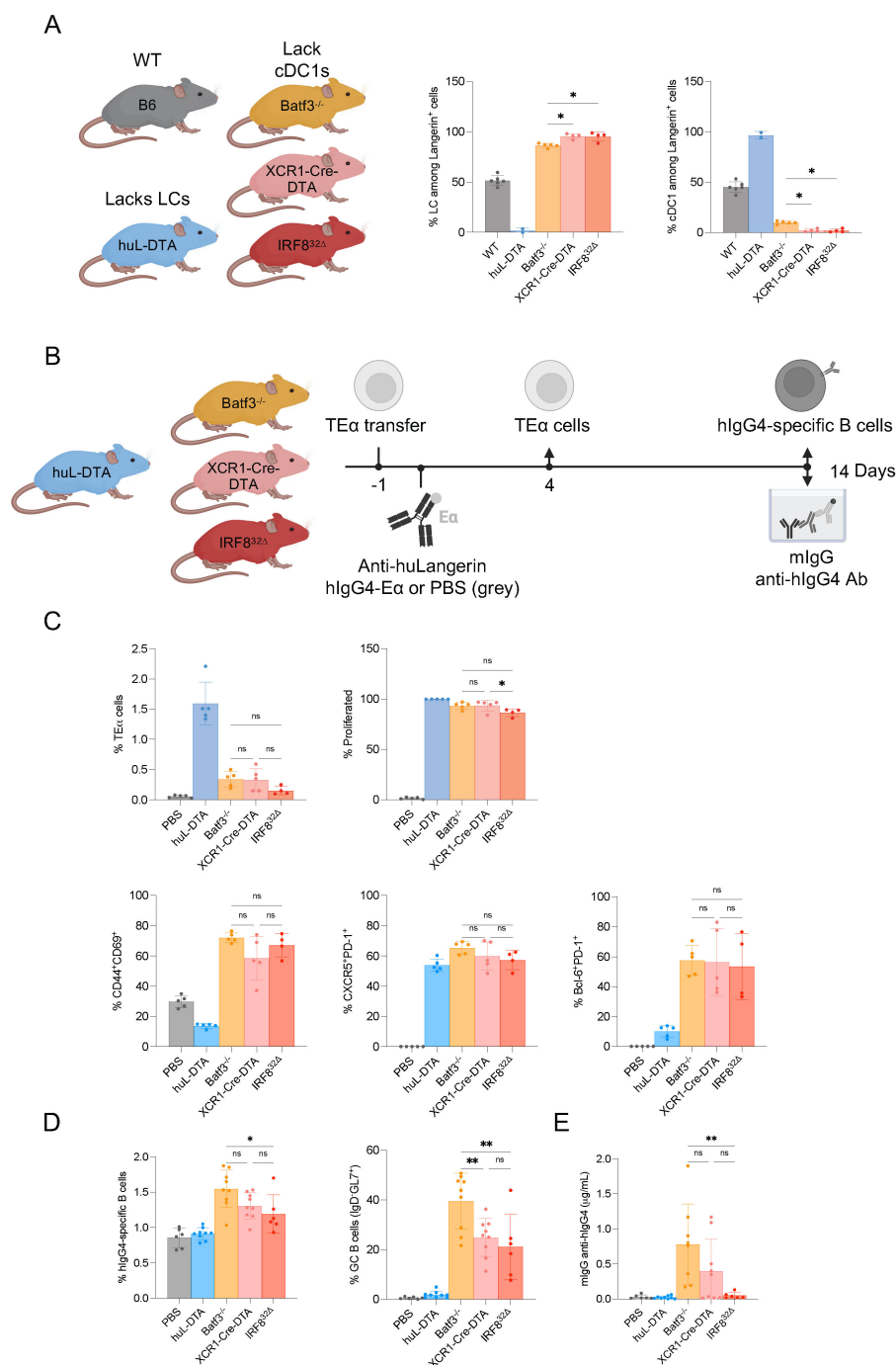


FIGURE 1

Langerhans cells (LCs), unlike cDC1s, induce germinal center T follicular helper (GC-Tfh) cells and antibody responses in steady-state. **(A)** LCs and cDC1s were quantified in the skin-draining lymph nodes of the indicated mouse strains. Data were pooled from two independent experiments. Each dot represents a separate mouse. **(B)** The indicated mice were transferred with TEα cells and then immunized with 1 μg of anti-muLangerin-hlgG4-Eα or vehicle (PBS) the next day. The antigen (Ag)-specific CD4<sup>+</sup> TEα cell responses were assessed by flow cytometry 4 days later **(C)**, while the Ag-specific B cell responses were characterized by flow cytometry **(D)** and the serum anti-hlgG4 levels by ELISA fourteen days later **(E)**. Data were pooled from two independent experiments. Each dot represents a separate mouse. \*p<0.05, \*\*p<0.005, ns=not significant.

which can address potential type-I interferon involvement in LC-induced adaptive immune responses in steady-state by acting directly on the T cells or indirectly through other cells. Again, we found no significant changes in T and B cell responses and a moderate increase rather than decrease or absence of anti-hlgG

antibody levels (Figures 2F, G). Thus, these data strongly support that the adaptive immune responses induced by steady-state LCs are largely independent of type-I interferon signaling.

Next, we tested whether exogenous IFNα could boost adaptive immune responses above the levels induced by steady-state LCs. For

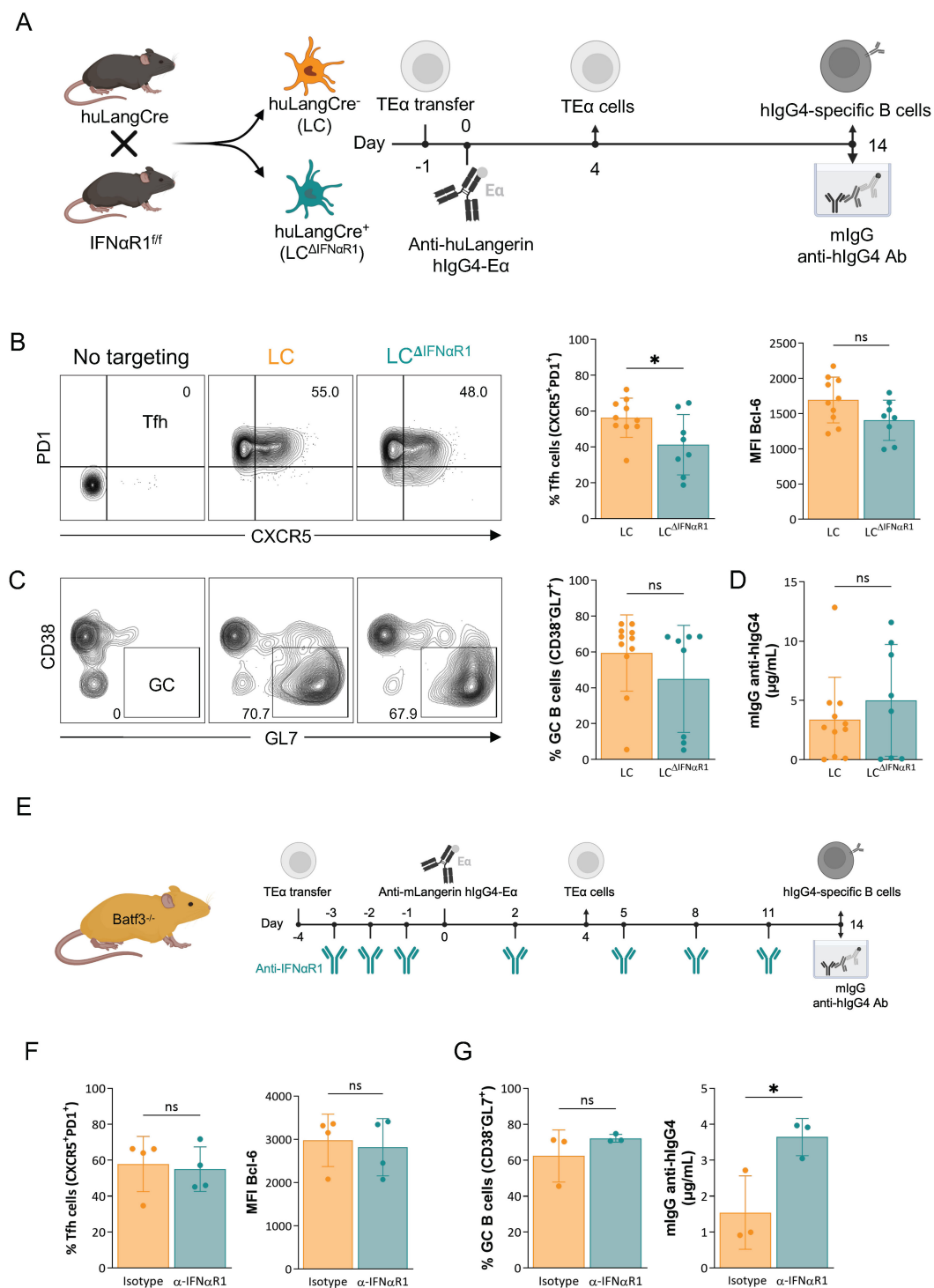


FIGURE 2

Type I interferon is not required for the induction of adaptive immune responses by steady-state LCs. **(A)** huLangCre-IFNαR1<sup>fl/fl</sup> mice were generated as depicted, which allowed us to target IFNαR1-deficient (LC<sup>ΔIFNαR1</sup>) or -sufficient LCs. These mice were transferred with TEα cells and then immunized with 1 μg of anti-huLangerin-hlgG4-Eα the next day. Ag-specific TEα cell responses were assessed 4 days later by flow cytometry. At fourteen days, flow cytometry and ELISA assessed Ag-specific B cell responses. **(B)** Representative contour plots of TEα cells with the percentage of Tfh cells (PD1<sup>+</sup>CXCR5<sup>+</sup>) and summary graphs, including Bcl-6 Mean Fluorescent Intensity (MFI) of the proliferated TEα cells. **(C)** Representative contour plots of Ag-specific B cells with percentage of GC B cells (CD38<sup>+</sup>GL7<sup>+</sup>) and summary graph. **(D)** hlgG4-specific mlgG serum levels defined by ELISA. Data from two independent experiments were pooled. Each dot represents a separate mouse. **(E)** The treatment plan of Batf3<sup>-/-</sup> mice with anti-IFNαR1 or isotype control antibody before and following LC targeting. **(F)** Left: the percentage of Tfh cells (PD1<sup>+</sup>CXCR5<sup>+</sup>) among proliferated TEα cells. Right: MFI of Bcl-6 of proliferated TEα cells. **(G)** Left: summary graph of Ag-specific GC B cells (CD38<sup>+</sup>GL7<sup>+</sup>), and right: hlgG4-specific mlgG serum levels defined by ELISA. Data from one representative experiment out of two is shown. Each dot represents a separate mouse. \*p<0.05, ns=not significant.

this, we used an anti-muLangerin-IFN $\alpha$  construct we previously described that enables cDC1 to support antibody responses (7). LCs, similarly to cDC1, express IFN $\alpha$ R (Supplementary Figure S2A). We found that delivering IFN $\alpha$  to LCs did not significantly alter their ability to support B cell responses (Supplementary Figure S2C). In total, these data show that modulation of type I IFN signaling in LCs does not impact their ability to support adaptive immune responses in this targeting model.

## IL-6 is not required for the induction of adaptive immune responses by steady-state LCs

IL-6 in mice, according to some but not all reports, plays a critical role in supporting the differentiation of Tfh cells in inflammatory models (22). However, its role in Tfh cell and antibody response induction in a steady-state is unknown. Steady-state LCs, unlike cDC1s, contain high levels of IL-6 mRNA transcript (7). Since LCs, but not cDC1s, can induce Tfh cells with germinal center (GC) phenotype (Bcl-6<sup>high</sup>) and protective antibody responses in steady-state models (6, 7), we hypothesized that LC-derived IL-6 might be essential in supporting the adaptive immune responses. To test this and limit IL-6 deficiency to LCs, we bred the IL-6<sup>lfl</sup> mice (32) to the huLangerinCre mice (33) (Figure 3A). The resulting genotypes were determined using PCR, and the selective genomic recombination of the IL-6 locus in LCs was confirmed using PCR on sorted cells (Supplementary Figure S2D). We then tested whether LC-derived IL-6 is needed to induce Tfh cells and antibody responses. The mice were transferred with transgenic CD4<sup>+</sup> TE $\alpha$  cells and then injected with 1  $\mu$ g of anti-huLangerin-E $\alpha$  intraperitoneally, as described above. Cre-negative IL-6<sup>lfl</sup> littermate mice served as controls. The mice were sacrificed 4 and 14 days later to characterize antigen-specific CD4<sup>+</sup> T cell and B cell responses as presented above (Figure 3A). The expansion and phenotype of TE $\alpha$  cells in the absence of LC-derived IL-6 remained unchanged (Figure 3B). The B cell responses, including GC cells and anti-hIgG IgG serum levels, showed no significant changes (Figure 3C). Thus, these data support the idea that LC-derived IL-6 is not required to support steady-state adaptive immune responses.

To rule out the possibility that IL-6 produced and secreted by bystander cells might aid the induction of adaptive immune responses by steady-state IL-6 deficient LCs, we performed IL-6 blocking experiments. Batf3<sup>-/-</sup> mice were treated with anti-IL-6 or isotype antibodies throughout the experiment (Figure 3D). Luminex<sup>®</sup> assay on serum samples was used to confirm the efficiency of IL-6 blockade (Supplementary Figure S2E). The antibody-treated Batf3<sup>-/-</sup> mice that lack cDC1s were adoptively transferred with CD4<sup>+</sup> TE $\alpha$  cells and then injected with 1  $\mu$ g of anti-muLangerin-E $\alpha$ , and then T and B cell responses were assessed as presented above. We found no significant differences in antigen-specific CD4<sup>+</sup> T cell and B cell expansions and phenotype (Figures 3D–F). The anti-huIgG IgG ELISA on serum samples revealed only a moderate decrease in antibody levels in the anti-IL-6 treated mice (Figure 3G). Thus, cumulatively, our experiments

showed that neither LC-derived nor total IL-6 plays a critical role in the induction of adaptive immune responses by steady-state LCs.

## ICOS-ICOS-L signaling has no major role in the induction of adaptive immune responses by steady-state LCs

Since steady-state levels of IL-6 and type-I interferon had no significant role in inducing adaptive immune responses by LCs, we turned our attention to membrane-bound co-stimulation. ICOS-ICOS-L signaling, including on DCs, is required to induce Tfh cells and subsequent antibody responses in inflammatory settings (34–36). To determine whether ICOS-ICOS-L interaction is involved in the induction of Tfh cells and antibody responses by steady-state LCs, we exposed Batf3<sup>-/-</sup> mice to ICOS-L blocking or isotype control antibodies (Figure 4A; Supplementary Figure S2F). The antigen-specific CD4<sup>+</sup> T cell and B cell responses were characterized as discussed above. We found that blocking ICOS signaling minimally reduced the GC B cell but not antibody responses and did not affect the induction of GC-Tfh cells by steady-state LCs (Figures 4B, C). Thus, these data indicate that ICOS signaling is not critical in inducing adaptive immune responses by steady-state LCs.

## CD80/CD86 on DCs are critical for the induction of adaptive immune responses by steady-state DCs

Since the inflammatory cytokines and co-stimulation previously identified as critical for Tfh differentiation and antibody responses had no significant role in inducing adaptive immune responses by steady-state LCs, we decided to establish an *in vitro* steady-state model to more efficiently test for DC-derived factors involved in the induction of the adaptive responses. For this *in vitro* platform, we used the MutuDC1 DC cells line (37), OT-II cells from a Rag2<sup>-/-</sup> background, and polyclonal primary B cells isolated from WT naïve mice (Figure 5A). The DCs and B cells were pulsed with OVA-peptide before co-culture, while cells not exposed to OVA served as controls. We anticipated that pulsing the polyclonal B cells with OVA-peptide should allow the cognate interaction with OT-II cells. Through this interaction, we expected that the B cells would provide the final maturation signals for the OT-II cells to differentiate into Tfh cells. In return, the T cells would facilitate the B cell responses, including isotype switching and antibody production. Indeed, we found that in the co-cultures where the DCs and the B cells were pulsed with OVA-peptide, the OT-II cells efficiently proliferated and differentiated into Tfh cells (Figure 5B). We also observed that a significant proportion of B cells underwent isotype switching and acquired GC phenotype (Figure 5C). We also detected substantial amounts of secreted IgG in the supernatant (data not shown). As expected, the inclusion of blocking MHC-II antibodies in the co-cultures prevented the T and B cell responses (Supplementary Figures S3A, B). Furthermore, the primary DCs and MutuDC2 DC cell line (38)



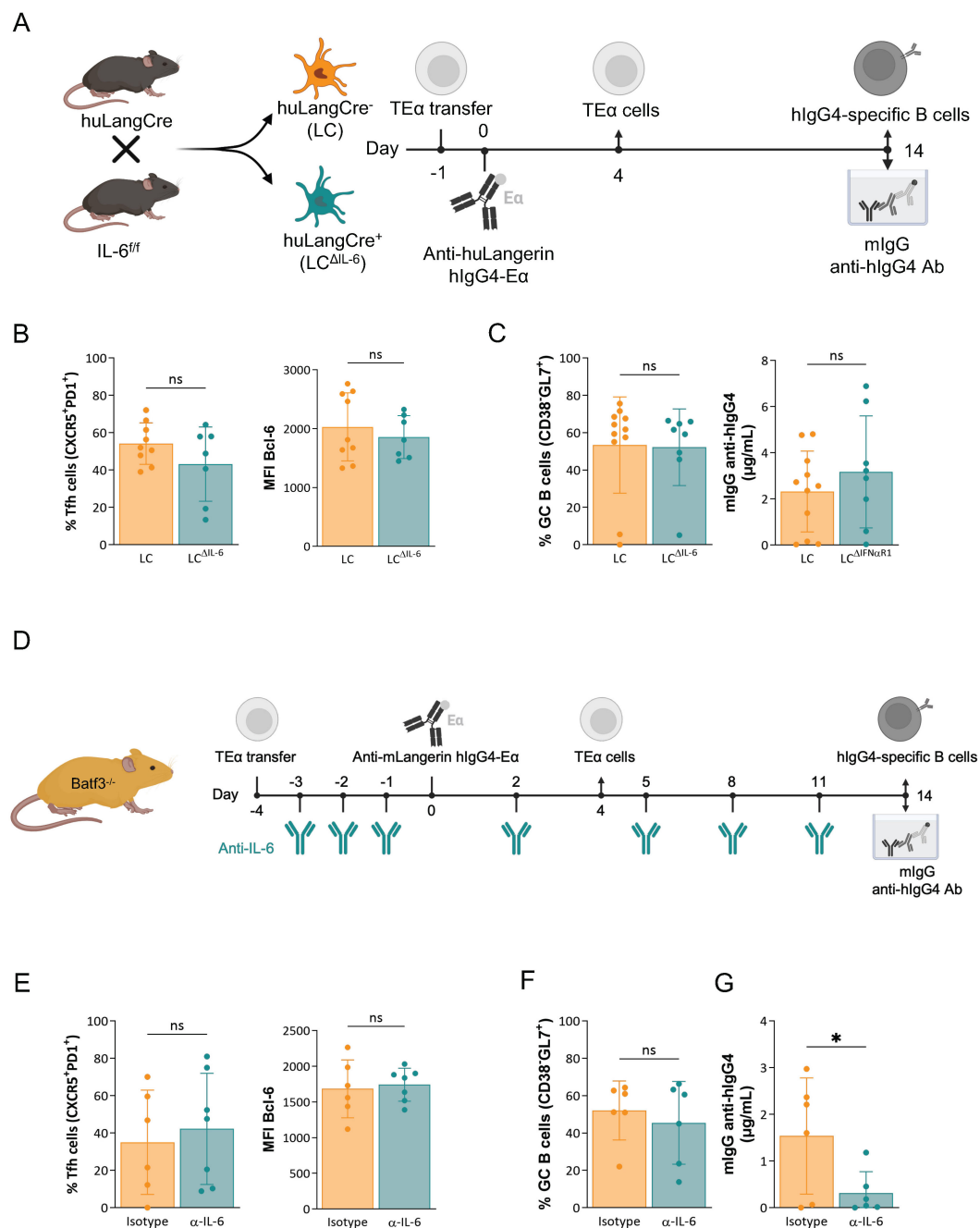


FIGURE 3

IL-6 is not required for the induction of adaptive immune responses by steady-state LCs. **(A)** *huLangCre*-*IL-6<sup>fl/fl</sup>* mice were generated as depicted, which allowed targeting either IL-6-deficient (*LC<sup>ΔIL-6</sup>*) or IL-6-sufficient LCs. These mice were transferred with TEα cells and then immunized with 1 μg of anti-huLangerin-hlgG4-Eα the next day. Ag-specific TEα cell responses were assessed 4 days later by flow cytometry. At fourteen days, flow cytometry and ELISA assessed Ag-specific B cell responses. **(B)** Summary graphs on the percentage of Tfh cells (PD1<sup>+</sup>CXCR5<sup>+</sup>) and Bcl-6 MFIs of the proliferated TEα cells. **(C)** Summary graph on Ag-specific GC B cell percentages (CD38<sup>+</sup>GL7<sup>+</sup>), and hlgG4-specific mlgG serum levels defined by ELISA. Data from two independent experiments were pooled. Each dot represents a separate mouse. **(D)** The treatment plan of *Batf3<sup>-/-</sup>* mice with anti-IL-6 before and following LC targeting. **(E)** Left: the percentage of Tfh cells (PD1<sup>+</sup>CXCR5<sup>+</sup>) among proliferated TEα cells. Right: MFI of Bcl-6 of proliferated TEα cells. **(F)** Summary graph of Ag-specific GC B cells (CD38<sup>+</sup>GL7<sup>+</sup>) and **(G)** hlgG4-specific mlgG serum levels defined by ELISA. Data from one representative experiment out of two is shown. Each dot represents a separate mouse. \*p < 0.05, ns = not significant.

in this co-culture assay also supported T and B cell responses but with different efficiencies (data not shown). Thus, we successfully established a steady-state co-culture system to study the induction of Tfh and B cell responses by DCs *in vitro*.

Having established the steady-state co-culture system, we next tested whether membrane-bound costimulatory molecules are involved in the T and B cell responses. We supplemented the co-cultures with blocking antibodies targeting CD40L (CD154), CD80/

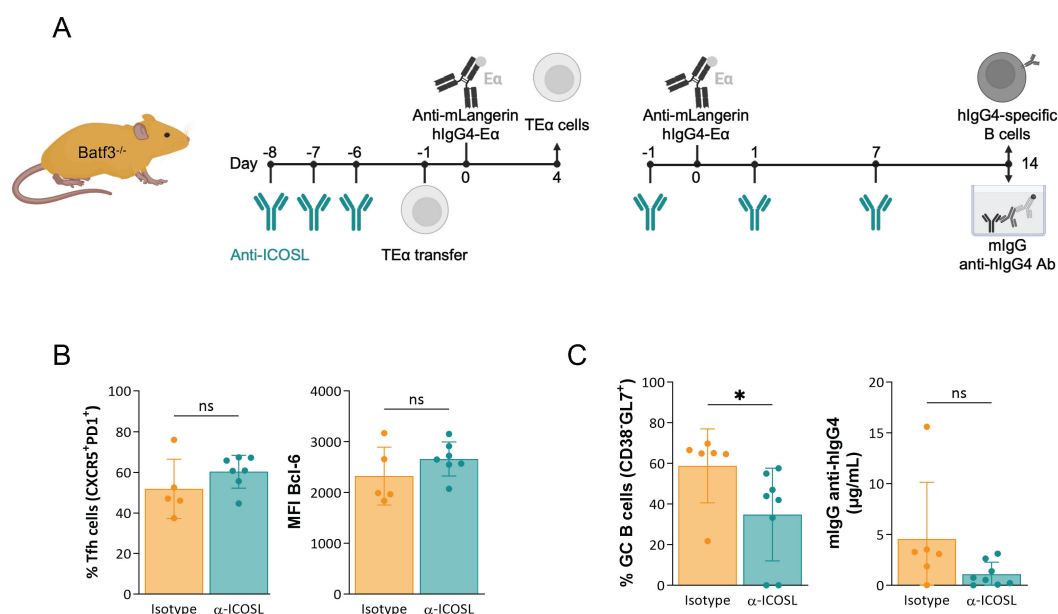


FIGURE 4

ICOS-ICOS-L signaling has no major role in the induction of adaptive immune responses by steady-state LCs. **(A)** The treatment plan of *Batf3*<sup>-/-</sup> mice with anti-ICOS-L before and following LC targeting to assess T- (left) and B cell responses (right). **(B)** Left: the percentage of Tfh cells (PD1<sup>+</sup>CXCR5<sup>+</sup>) among proliferated TEα cells. Right: MFI of Bcl-6 of proliferated TEα cells. Data from one representative experiment out of three is shown. **(C)** Left: summary graph of Ag-specific GC B cells (CD38<sup>+</sup>GL7<sup>+</sup>), and right: hlgG4-specific mlgG serum levels defined by ELISA. Data from two independent experiments were pooled. Each dot represents a separate mouse. \**p*<0.05, ns=not significant.

CD86, and ICOS-L (CD275) to test. We observed that blocking CD80 and CD86, but not the others, significantly inhibited the differentiation of Tfh cells and class-switched (GL7<sup>+</sup>IgD<sup>+</sup>) B cell responses (Figures 5B, C; Supplementary Figures S3A, B). Thus, CD80 and CD86 are critical in adaptive responses induced by steady-state DCs *in vitro*.

To confirm that CD80 and CD86 are also crucial in LC-induced responses *in vivo*, we repeated our LC-targeting experiments presented above in the presence of anti-CD80/CD86 or corresponding isotype antibodies (Figure 5D). We found that antibodies blocking CD80/CD86 signaling *in vivo* significantly inhibited the induction of Tfh cells by LCs (Figure 5E) and entirely suppressed B cell responses, including GC formation and antibody production (Figure 5F). Thus, membrane-bound co-stimulation through CD80/CD86 is critical for steady-state LC-induced adaptive immune responses.

In inflammatory settings, CD80/CD86 on DCs, but not on B cells, are required for adaptive T and B cell responses (39). To define whether those findings also apply to our steady-state antigen targeting model, we first used our *in vitro* co-culture assay presented above with slight modification. We co-cultured magnetically enriched migratory DCs from the SDLNs of WT or CD80/CD86 double knock-out (DKO) mice pulsed with anti-muLangerin-OVA or IgG4-OVA with OT-II T cells and WT or CD80/CD86 double knock-out B cells (Supplementary Figures S3C, D). The Tfh cell differentiation was unaffected by the lack of CD80/CD86 on the B cells but was almost absent in cultures with DCs that lacked CD80/CD86 (Figure 5G). These data, therefore, support the idea that CD80/CD86 expression by DCs plays a critical role in the induction of Tfh cell responses.

## Discussion

In summary, we demonstrate that Langerhans cells (LCs) promote GC-Tfh and B cell responses in steady-state, independent of IL-6, type-I interferon, and ICOS signaling. However, we found that CD80/CD86 expression on DCs is essential for inducing these adaptive immune responses. These findings differentiate steady-state T cell differentiation from the conventional three-signal model of T cell differentiation in inflammatory settings, where cytokines are indispensable third signals.

The induction of humoral immune responses in the steady-state is not exclusive to LCs. Splenic cDC1s have also been reported to support Tfh and antibody responses, though their ability to do so, unlike LCs', depends on the receptor targeted (40). In previous experiments, targeting migratory skin cDC1s through Langerin and Dectin-1 failed to elicit GC-Tfh or B cell responses, instead promoting cells with a pre-Tfh/Th1 phenotype (7). The reasons for these differences—whether due to distinct cDC1 subsets residing in different tissues (e.g., lymph nodes vs. spleen) or specific receptor targeting—remain to be elucidated. It will be crucial to investigate the instances when the cDC1s can support antibody responses, whether they undergo receptor-dependent alterations akin to those induced by inflammatory cues, such as IFN-α or poly(I:C) (7). As previously observed, the pre-Tfh/Th1 responses induced by combined targeting of LCs and cDC1s via Langerin in steady-state were also independent of type-I interferons and IL-6 (6), further reinforcing that adaptive immune responses induced by

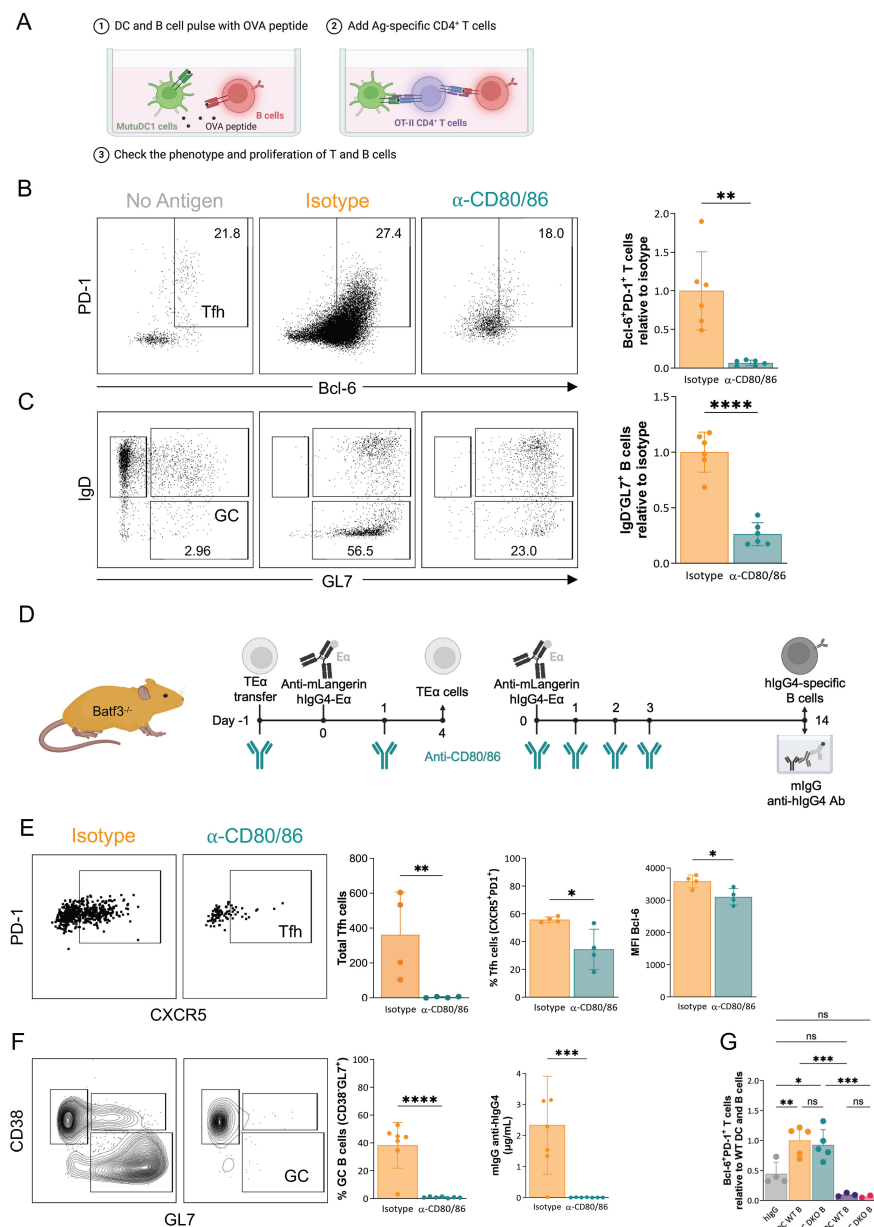


FIGURE 5

CD80/CD86 on DCs are critical for the induction of adaptive immune responses by steady-state DCs. **(A)** *In vitro* steady-state platform to model GC-dependent adaptive immune responses. (1) Murine DC cells (MutuDC1 cell line) were pulsed with OVA peptide. (2) Ag-specific CD4<sup>+</sup> T cells (OT-II) were added after washing off the peptide. (3) After 5 days, the phenotype of T and B cells was determined by flow cytometry. **(B)** The role of CD80/86 in adaptive immune responses was tested *in vitro*. Anti-CD80/86 blocking Ab (or an isotype control Ab) were added simultaneously with T cells. Five days later, the phenotype of T cells was assessed by flow cytometry. Representative dot plot of proliferated OT-II cells with percentage of Tfh cells (PD1<sup>+</sup>Bcl-6<sup>+</sup>). Summary graph: the number of Tfh cells in each well was calculated and plotted relative to the average of Tfh cells in isotype conditions. Data from two independent experiments were pooled. Each dot represents a separate replicate. **(C)** Representative dot plot of proliferated B cells with percentage of GC cells (IgD<sup>+</sup>GL7<sup>+</sup>). Summary graph: the number of GC B cells in each well was calculated and plotted relative to the average of GC B cells in isotype conditions. Data from two independent experiments were pooled. Each dot represents an independent replicate. **(D)** The treatment plan of Batf3<sup>-/-</sup> mice with anti-CD80/CD86 before and following LC targeting to assess T- (left) and B cell responses (right). **(E)** Representative TEα flow plots and summary graphs. Left: Total Tfh cells. Middle: The percentage of Tfh cells (PD1<sup>+</sup>CXCR5<sup>+</sup>) among proliferated TEα cells. Right: MFI of Bcl-6 of proliferated TEα cells. Data from one representative experiment out of three is shown. Each dot represents a separate mouse. **(F)** Representative flow plots and summary graphs for antigen-specific B cells. Left: summary graph of Ag-specific GC B cells (CD38<sup>+</sup>GL7<sup>+</sup>), and right: hlgG4-specific mlgG serum levels defined by ELISA. Data from two independent experiments were pooled. Each dot represents a separate mouse. **(G)** To test the role of CD80/86 on DCs and B cells, DCs and B cells were isolated from WT or CD80/86 DKO mice. DCs and B cells were pulsed for 24h with OVA peptide attached to an anti-mLangerin Ab (or non-targeted Ab (hlgG)). Then, after washing, Ag-specific OT-II T cells were added. After 5 days, the phenotype of T cells was checked by flow cytometry. The number of Tfh cells in each well was calculated and plotted relative to the average Tfh cells in WT DC/WT B cell conditions. Data from two independent experiments were pooled. Each dot represents an independent replicate. \*p<0.05, \*\*p<0.005, \*\*\*p<0.001, \*\*\*\*p<0.0001, ns=not significant.



DCs in steady-state are independent of these cytokines. Notably, in our model, no polarizing adjuvants or pattern recognition ligands were used that could directly or indirectly differentially affect LCs and cDC1s. Both subsets were targeted via the same receptor, yet they induced distinct adaptive immune responses. This strongly supports the idea that DC subsets are functionally specialized or pre-programmed, even in steady-state, to drive specific adaptive immune responses. Our findings align with studies on pre-committed DC precursors in the bone marrow (41, 42) and human *in vitro* observations that both primary tissue- and CD34<sup>+</sup> cord-blood-derived LCs, but not monocyte-derived DCs support Tfh and B cell responses in steady-state (7, 15), suggesting that tissue residency might play a limited role in shaping the functional specialization of DC subsets. Also, these results underscore the intrinsic programming of DC subsets in directing distinct immune pathways and, at the same time, highlight the translatability of mouse data to humans.

The findings that these prominent immunological factors in defining Tfh cell differentiation and B cell responses in our model do not seem to be critical contributors do not rule out that other cytokines or soluble/membrane-bound factors might play a significant role in the process. However, our observations may offer insight into the mechanisms underlying homeostatic immunity toward commensals (16) and the development of certain autoimmune diseases. Engagement of DCs by commensals through pattern recognition receptors, unlike pathogenic interactions, typically leads to no detectable or minimal activation and maturation (43), suggesting limited involvement of DC-derived cytokines in polarizing commensal-specific T helper (Th) subsets. If cytokines are not critical in steady-state, what drives distinct Th responses? One possibility is that DC subsets differ in their peptide-MHC levels, a hypothesis aligned with the quantitative model proposed by van Panhuys and colleagues (44). However, our findings suggest that additional factors beyond peptide-MHC levels contribute to Tfh and B cell responses. LCs, across a wide range of antigen doses, while with different efficiency, uniquely support antibody responses (6, 7), unlike cDC1s, which fail to do so under similar conditions. LCs appear to provide stronger cumulative TCR stimulation, evidenced by sustained CD69 expression, pS6 phosphorylation (7), and Nur77-GFP signals (unpublished observation) in T cells activated by LCs. Given that Tfh differentiation requires stronger TCR stimulation than Th1 differentiation (45), this enhanced signal may explain the unique ability of LCs to promote Tfh cells. How LCs provide more potent stimuli than cDC1s and drive distinct adaptive immune responses in steady-state and inflammation (25) remains to be determined. While here we show that CD80/CD86 play an essential role in LC-induced adaptive immune responses, the contribution of CD80/CD86 as the second signal is likely not unique to LCs since other DCs in the lymph nodes also express high levels of CD80/CD86. Thus, other factors unique to these DC subsets, such as differentially expressed CD11a and CD11b integrins (7), molecules that play an essential role in regulating immunological synapses (46, 47), could likely serve as the decisive “third signal” and polarize the naïve T cells into distinct Th cells.

LCs and cDC1s exhibit distinct cytokine transcript profiles in the steady state, which may underlie their functional specialization (25). LCs are enriched in transcripts for *Il1b*, *Il6*, and *Il23p19*, aligning with their capacity to promote Th17 responses. Conversely, cDC1s harbor higher levels of *Il12p40* and *Il27* transcripts, correlating with their roles in driving Th1 and CTL responses. Interestingly, *Il12p40* transcript expression is detectable even in pre-committed bone marrow cDC1 precursors (42), indicating intrinsic programming that primes DCs for rapid and specific cytokine production upon activation. These findings suggest that DC subsets are poised to respond swiftly to external stimuli by producing subset-specific cytokines that facilitate targeted Th polarization. However, our steady-state results indicate that cytokines may not be involved in the polarization of Th cells under non-inflammatory conditions. Therefore, we propose a model wherein, in the steady-state differential expression of adhesion molecules—such as integrins (CD11a and CD11b)—by DC subsets, in combination with distinct peptide/MHC levels, may provide a critical “third signal” to skew adaptive immune responses. These interactions of different strengths could selectively promote “basic” Tfh, Th1, and potentially Th2 differentiation without the need for cytokine-mediated signaling. Under inflammatory conditions, cytokines would act as a “fourth signal,” boosting and further polarizing the T helper cells into effector subsets, such as Th17, Th22, and others, tailored to combat the specific infection and restore tissue homeostasis. This dual-layered model highlights how DC subsets integrate their intrinsic programming with environmental cues to orchestrate adaptive immunity dynamically.

## Materials and methods

### Mice

huLangerin (also called huLangerin-DTR) (24), Batf3<sup>-/-</sup> (48), and huLangerinCre (33) mice have been previously described. huLangerinCre were crossed with IFN $\alpha$ R1<sup>f/f</sup> (Jackson Laboratories strain 028256) or IL-6<sup>f/f</sup> (mice provided by Dr. Roger Davis, University of Massachusetts; developed by Dr. Juan Hidalgo at Universitat Autònoma de Barcelona) (32). CD90.1 congenic TE $\alpha$  Rag1<sup>-/-</sup> CD4 TCR transgenic mice to I-E $\alpha$ <sub>52–68</sub> on the C57BL/6 background were initially obtained from Dr. Marc Jenkins (University of Minnesota). IRF8<sup>32 $\Delta$</sup>  mice were obtained from Dr. Kenneth Murphy (Washington University School of Medicine) and Jackson Laboratories. XCR1-Cre-DTA mice were generated by crossing XCR1-Cre (Jackson Laboratories strain 035435; developed by Dr. Kenneth Murphy) with “STOP”-DTA (Jackson Laboratories strain 009669). WT C57BL/6J (strain 000664), CD45.1 PepBoy (strain 002014), and OT-II (strain 005194) were purchased from Jackson Laboratories and maintained in our facility. Rag2<sup>-/-</sup> OT-II mice were purchased from Taconic model 11490. CD80/86 double knock-out (DKO) mice developed by Dr. Arlene H. Sharpe (Mass General Hospital and Harvard Medical School) (49) was provided by Drs. Masashi Watanabe and Richard Hodes (NIH). All experiments were

performed with 6- to 12-week-old female and male mice. Mice were housed in microisolator cages and fed autoclaved food and water. The Institutional Care and Use Committee at Thomas Jefferson University approved all mouse protocols under protocol number: 02315.

## Steady-state Langerin targeting

These experiments were performed with anti-human/anti-mouse mAb and conjugates (anti-huLangerin-E $\alpha$ , anti-muLangerin-E $\alpha$  anti-muLangerin-doc, cohesin-IFN $\alpha$ 4) generated in-house, as previously described (7). All the reagents used in this study were generated using mammalian cell lines to minimize the presence of endotoxins. The average endotoxin level was below 0.2 ng LPS/mg protein. E $\alpha$  (I-E $\alpha$ <sub>52-68</sub>) is a well-characterized immunodominant T cell epitope from the I-E $\alpha$  MHCII molecule recognized by transgenic TE $\alpha$  cells in the context of I-A $\beta$ . For the generation of the anti-muLangerin-IFN $\alpha$ 4 construct, we used a previously described technology that relies on the high-affinity interactions between dockerin (doc) and cohesin (coh) (7). Dockerin was fused to the heavy chain of the antibody. Mice received intravenous (i.v.) transfer of CFSE-labeled, congenically marked 3x10<sup>5</sup> TE $\alpha$  cells 1 day before antigen targeting as previously described (7). One  $\mu$ g of anti-human/anti-mouse mAb and conjugates or PBS were administered intraperitoneally (i.p.) on day 0. For TE $\alpha$  cells characterization, mice were sacrificed 4 days after Langerin targeting, and the skin-draining lymph nodes (SDLNs; axillary, brachial, and inguinal) were harvested for flow cytometry. For B cell characterization, mice were sacrificed on day fourteen, the SDLNs were harvested for flow cytometry, and the blood was collected for serum isolation and ELISA. For dendritic cell characterization, SDLNs were digested as described previously (7) before staining for flow cytometry.

## Flow cytometry

Flow cytometry was performed on single-cell suspensions of the SDLNs (axillary, brachial, and inguinal) of mice. The fixable viability dye (Thermo Fisher Scientific) was used to exclude dead cells. The following antibodies from BioLegend were used to stain cells CD3 (145-2C11), CD4 (GK1.5), CD16/CD32 (93), CD19 (6D5), CD25 (PC61), CD44 (IM7), CD45.2 (104), CD69 (H1.2F3), CD80 (16-10A1), CD86 (GL-1), CD90.2 (30-H12), CD138 (281-2), CD275 (HK5.3), B220 (RA3-6B2), Blimp1 (5E7), CXCR5 (L138D7), GL7 (GL7), IFN $\alpha$ R1 (MAR1-5A3), IgD (11-26c.2a), IgM (RMM-1), MHCII (M5/114.15.2), PD-1 (29F.1A12), and Sca1 (D7). CD4 (GK1.5), CD38 (90), CD90.1 (OX-7), Bcl6 (K112-91), and IgD (D7) were purchased from BD Biosciences. CD11b (M1/70), CD90.2 (53-2.1), F4/80 (BM8) were purchased from Thermo Fisher Scientific. For antigen-specific B cell staining, cells were also incubated *ex vivo* with AF647-conjugated huIgG4. Intracellular transcription factor staining was performed with the BD Bioscience Cytofix/Cytoperm kit (BD Biosciences, San Jose,

CA), according to the manufacturer's instructions. All the flow cytometric plots presented in this article were pre-gated on live (using Live/Dead stain) and singlet events. Samples were analyzed on an LSRFortessa or Symphony flow cytometer (BD Biosciences), and data were analyzed with FlowJo software (BD Biosciences).

## Assessment of humoral immune responses by ELISA

Serum samples were obtained 14 days after immunization with anti-Langerin Ab constructs using BD Microtainer SST tubes (BD) and stored at  $-80^{\circ}\text{C}$ . The targeting antibodies used in our study are based on a human IgG4 framework, and we assess anti-huIgG4 responses as a surrogate readout of humoral immunity to the targeting construct. To determine antigen-specific antibody titers, clear flat-bottom immune 96-well plates were coated with 50  $\mu$ L of huIgG4 protein diluted in BupH Carbonate-Bicarbonate buffer (Thermo Fisher Scientific) at 2  $\mu$ g of protein/ml and incubated overnight at  $37^{\circ}\text{C}$ . After washing, plates were blocked with blocking buffer (TBS; Thermo Fisher Scientific). After blocking, the buffer was discarded, and serial dilutions of serum in the blocking buffer were added and incubated for 2 h at  $37^{\circ}\text{C}$ . A serial dilution of a mouse anti-hIgG4 antibody (EMD Millipore) was used as a standard. After washing, plates were incubated with horseradish peroxidase (HRP)-conjugated goat anti-mouse IgG (Jackson ImmunoResearch; West Grove, PA) in blocking solution for 2 h at  $37^{\circ}\text{C}$ , washed and developed with HRP substrate (Ultra-TMB Chromogen Solution: ThermoFisher Scientific). The reaction was stopped with 1N HCl and plates were read at 450 nm.

## IFN $\alpha$ R1 antibody *in vivo* treatment

For blockade of IFN $\alpha$ R1, Batf3<sup>-/-</sup> mice were treated with 0.5 mg/mouse of IFN $\alpha$ R1 blocking antibody (clone MAR1-5A3; BioLegend) on 3 consecutive days pre-immunization and 0.25 mg every 3 days post-immunization (50). Control mice received a similar amount of a mouse IgG1 isotype control antibody (clone MOPC-21; BioLegend). All antibodies were administrated i.v. in 300  $\mu$ L of PBS. To validate the block, SDLNs were isolated and stained for IFN $\alpha$ R1 (the same clone used *in vivo* to block the receptor).

## IL-6 antibody *in vivo* treatment

For the blockade of IL-6, Batf3<sup>-/-</sup> mice were treated with 0.5 mg/mouse of IL-6 blocking antibody (clone MP5-20F3; BioLegend) on one-day pre-immunization and 0.25 mg every other day post-immunization. Control mice received a similar amount of a rat IgG1 isotype control antibody (clone RTK2071; BioLegend). All antibodies were administrated i.v. in 300  $\mu$ L of PBS. To validate the block, the blood of each mouse was collected, and serum was isolated for Luminex<sup>®</sup> analysis.

## ICOS-L antibody *in vivo* treatment

For blockade of ICOS-L (CD275) and TE $\alpha$  cell characterization, Batf3<sup>-/-</sup> mice were treated with 0.1 mg/mouse of ICOS-L blocking antibody (clone HK5.3; BioLegend) on days -8, -7, and -6 pre-immunization. CFSE-labeled TE $\alpha$  cells were transferred on day -1. Control mice received a similar amount of a rat IgG2a isotype control antibody (clone RTK2758; BioLegend). All antibodies were administrated i.v. in 300  $\mu$ l of PBS. For blockade of ICOS-L (CD275) and B cell characterization, Batf3<sup>-/-</sup> mice were treated with 0.1 mg/mouse of ICOSL blocking antibody (clone HK5.3; BioLegend) on day -1 pre-immunization, and days 1 and 7 post-immunization. Control mice received a similar amount of a rat IgG2a isotype control antibody (clone RTK2758; BioLegend). All antibodies were administrated i.v. in 300  $\mu$ l of PBS. To validate the block, the blood of each mouse was collected and stained for ICOS-L with the exact clone as the antibody used for the *in vivo* treatment.

## CD80/86 antibodies *in vivo* treatment

For blockade of CD80 and CD86 and TE $\alpha$  cell characterization, Batf3<sup>-/-</sup> mice were treated with 0.15 mg/mouse of CD80 (clone 16-10A1; BioXCell) and 0.15 mg/mouse of CD86 (clone GL-1; BioXCell) blocking antibodies on days -1, 0, and 1 (relative to immunization day). Control mice received a similar amount of a rat IgG2a isotype control antibody (clone RTK2758; BioLegend). All antibodies were administrated i.p. in 100  $\mu$ l of PBS. For blockade of CD80 and CD86 and B cell characterization, Batf3<sup>-/-</sup> mice were treated with 0.15 mg/mouse of CD80 (clone 16-10A1; BioXCell) and 0.15 mg/mouse of CD86 (clone GL-1; BioXCell) blocking antibodies on days 0, 1, 2 and 3. Control mice received rat IgG2a and Armenian hamster IgG isotype control antibodies (clones 2A3 and BE0091, respectively; BioXCell). All antibodies were administrated i.p. in 100  $\mu$ l of PBS. SDLNs were stained with CD80 and CD86 antibodies to validate the block (same clone as the antibodies used for the *in vivo* treatment).

## *In vitro* assay with MutuDC1

For this assay, we combined and optimized protocols from P. Sage and A. Sharpe (51) and Kolenbrander et al. (52).

Cells were prepared in co-culture in 96-well U-bottom plate as follows: 1) 10<sup>4</sup> MutuDC1 cells/well were distributed in complete IMDM (IMDM w/Glutamax w/HEPES, 8% Heat-inactivated FBS, 50  $\mu$ M  $\beta$ -mercaptoethanol and 1% pen/strep). 2) B cells were labeled with Cell-Trace Yellow (BioLegend) and enriched (Mojosort pan-B cell selection kit from BioLegend) from the spleen of CD45.1 mice. 2.5x10<sup>5</sup> CD45.1 B cells were distributed in the same wells as MutuDC1. 3) MutuDC1 and B cells were pulsed at 15  $\mu$ g/mL with OVA<sub>323–339</sub> peptide (GenScript) for 1 hour at 37°C 5% CO<sub>2</sub>. 4) Rag2/OT-II T cells were isolated from spleen, mesenteric and SDLNs and labeled with Cell-Trace Violet (BioLegend). After washing MutuDC1 and B cells with complete

IMDM twice, 5x10<sup>5</sup> Rag2/OT-II T cells were added per well. 5) After mixing, cells were incubated for 5 days at 37°C 5% CO<sub>2</sub>.

Different controls lacking different cell populations or peptides were used. If any blocking antibodies were added to wells, it was at the same time as the addition of T cells at 5  $\mu$ g/mL. Blocking antibodies used were MHC-II block (clone Y-3P from BioXCell), CD80 (clone 16-10A1 from BioLegend); CD86 (clone GL-1 from BioLegend); CD154 (clone MR1 from BioLegend); CD275 (clone HK5.3 from BioLegend). At the end of the incubation, the plate was centrifuged. The supernatant was used for ELISA mIg detection. Briefly, clear flat-bottom immune 96-well plates were coated with 50  $\mu$ L of F(ab')<sub>2</sub> Donkey anti-mouse IgG (H+L) (ThermoFisher Scientific) diluted at 8  $\mu$ g/mL in BupH Carbonate-Bicarbonate buffer (Thermo Fisher Scientific) and incubated overnight at 37°C. After washing with PBS + Tween20 (ThermoFisher Scientific), plates were blocked with a 2% milk solution for 30 minutes at 37°C. After washing, serial dilutions of supernatant in TBS were added and incubated for 2 h at 37°C. After washing, plates were incubated with horseradish peroxidase (HRP)-conjugated Donkey anti-mouse IgG (H+L) (ThermoFisher Scientific) in TBS for 2 h at 37°C, washed and developed with HRP substrate (Ultra-TMB Chromogen Solution: ThermoFisher Scientific). The reaction was stopped with 1N HCl and plates were read at 450 nm.

The cells were stained with the following antibodies: CD4 (GK1.5; BD Biosciences), CD44 (IM7; BioLegend), CD45.1 (A20; BioLegend), PD1 (39F.1A12; BioLegend), Bcl6 (K112-91; BD Biosciences), GL7 (GL7; BioLegend), IgD (11-26c.2a; BioLegend), CD19 (6D5; BioLegend), CD16/30 (93; BioLegend), and a fixable live/dead from Thermofischer Scientific.

## *In vitro* assay with primary DCs

This assay is similar to the *in vitro* assay with MutuDC1 with the following differences. The primary DC fraction was a CD11c positive enrichment (Mouse CD11c positive selection kit II from StemCell) of SDLNs of WT and CD80/86 DKO mice. The T cell fraction is a CD4 T cell enrichment (Mojosort mouse CD4 T cell enrichment from BioLegend) of spleen mesenteric and SDLN of OT-II mice. The B cell fraction is a B cell enrichment (Mouse Pan-B cell enrichment from BioLegend) of WT and CD80/86 DKO mice spleens. The antigen used here is anti-muLangerin-doc/cohesin-OTII (and control IgG4-doc/cohesion-OTII) generated in-house, as previously described (7). Primary DC (5x10<sup>4</sup> cells) and B cell (10<sup>6</sup> cells) fractions were pulsed for 24 hours at 37°C 5% CO<sub>2</sub> with 10nM of the targeting or control constructs. After washing, 10<sup>5</sup> cells of the T cell fraction were added and incubated for 5 more days at 37°C 5% CO<sub>2</sub>.

The staining of the cells at the end of the co-culture assay included the following antibodies from BD Biosciences: CD4 (GK1.5), CD38 (90) and Bcl-6 (K112-91). ThermoFisher Scientific antibodies used were specific for MHCII (M5/114.15.2), CD4 (GK1.5), CD86 (GL1), and the fixable live/dead marker. The following antibodies were purchased from BioLegend: CD44 (IM7), CD45.1 (A20), CD138 (281-2), IgD (11-26c.2a), CD19 (6D5), GL7 (GL7), CD11c (N418), PD1 (29F.1A12), and CD16/32 (93).

## Statistical analysis

Differences between 2 data sets were analyzed first for normality using the Shapiro-Wilk test. If normality was met, an unpaired t-test was used to assess the difference between the 2 different data sets. In the absence of normality, a Mann-Whitney test was used. For data sets with more than two groups, an ordinary one-way ANOVA with multiple comparisons was used. All analysis were performed with GraphPad Prism software.

## Data availability statement

The original contributions presented in the study are included in the article/**Supplementary Material**. Further inquiries can be directed to the corresponding author.

## Ethics statement

The animal study was approved by The Institutional Care and Use Committee at Thomas Jefferson University. The study was conducted in accordance with the local legislation and institutional requirements.

## Author contributions

AB: Data curation, Formal analysis, Investigation, Methodology, Validation, Visualization, Writing – review & editing. ZQ: Data curation, Formal analysis, Investigation, Methodology, Validation, Visualization, Writing – review & editing. SZ: Investigation, Methodology, Resources, Writing – review & editing. GZ: Investigation, Methodology, Resources, Writing – review & editing. BI: Conceptualization, Funding acquisition, Project administration, Resources, Visualization, Writing – original draft, Writing – review & editing.

## Funding

The author(s) declare that financial support was received for the research and/or publication of this article. BZI is supported by the National Institute of Allergy and Infectious Diseases (<https://www.niaid.nih.gov>) R01AI146420 and institutional start-up funds.

## Acknowledgments

We thank the BioImaging Shared Resources, Flow Cytometry, and Laboratory Animal Facilities at Sidney Kimmel Cancer Center for their expert assistance in performing the presented experiments. We thank Dr. Hans Acha-Orbea for sharing the MutuDC cell lines. We thank Dr. Luis Sigal for sharing the IFN $\alpha$ R<sup>KO</sup> mice, Drs. Arlene Sharpe, Masashi Watanabe, and Richard Hodes for the

CD80/CD86<sup>DKO</sup> mice, Drs. Juan Hidalgo and Roger Davis for the IL-6 floxed mice, and Dr. Kenneth Murphy for the IRF8<sup>32Δ</sup> mice. Jerome Ellis and Zhiqing Wang are thanked for reagent making, and Jiukai Yu for laboratory assistance. Some of the figures were generated using BioRender. This work was supported by the National Institute of Allergy and Infectious Diseases (<https://www.niaid.nih.gov>) R01AI146420 to BI and institutional start-up funds. The Flow Cytometry and Laboratory Animal Facilities at Sidney Kimmel Cancer Center at Thomas Jefferson University are supported by the National Cancer Institute (<https://www.cancer.gov>) P30CA056036.

## Conflict of interest

The authors declare that the research was conducted in the absence of any commercial or financial relationships that could be construed as a potential conflict of interest.

The author(s) declared that they were an editorial board member of Frontiers, at the time of submission. This had no impact on the peer review process and the final decision.

## Generative AI statement

The author(s) declare that no Generative AI was used in the creation of this manuscript.

## Publisher's note

All claims expressed in this article are solely those of the authors and do not necessarily represent those of their affiliated organizations, or those of the publisher, the editors and the reviewers. Any product that may be evaluated in this article, or claim that may be made by its manufacturer, is not guaranteed or endorsed by the publisher.

## Supplementary material

The Supplementary Material for this article can be found online at: <https://www.frontiersin.org/articles/10.3389/fimmu.2025.1611812/full#supplementary-material>

### SUPPLEMENTARY FIGURE 1

LCs, unlike cDC1s, induce GC-Tfh cells and antibody responses in steady-state. (A) Gating strategy for LCs and cDC1s is shown on the left; representative flow cytometry plots from the indicated mouse strains are shown on the right. (B) Left: Gating strategy and phenotype of TE $\alpha$  cells. Right: Representative flow plots from the indicated mouse strains. (C) Left: Gating strategy and phenotype of antigen-specific B cells. Right: Representative flow plots from the indicated mouse strains. L/D = live/dead.

### SUPPLEMENTARY FIGURE 2

Validation experiments for type I interferon, IL-6, and ICOS-L interference. (A) huLangCre-IFN $\alpha$ R1<sup>f/f</sup> mice were generated to delete IFN $\alpha$ R1 in LCs specifically. SDLN of huLangCre-IFN $\alpha$ R1<sup>f/f</sup> mice (Cre+), littermate controls (Cre-) and IFN $\alpha$ R1 complete knockout (KO) mice were stained for IFN $\alpha$ R1 by flow cytometry. MFI of IFN $\alpha$ R1 was calculated for B cells, cDC1s, LCs, and



rDCs. Data from multiple experiments pooled together. Each dot represents a separate mouse. **(B)** *Batf3*<sup>-/-</sup> mice were treated with anti-IFN $\alpha$ R1 blocking Ab or an isotype. Four and fourteen days after LC targeting, SDLN were isolated and stained for IFN $\alpha$ R1 (same clone used *in vivo* to block the receptor). Left: representative histogram of B cells from isotype or anti-IFN $\alpha$ R1 treated mice. Shaded grey are B cells stained with an isotype control. Right: summary data of IFN $\alpha$ R1 staining on B cells. **(C)** LCs were targeted with 1  $\mu$ g of anti-mLangerin-hlgG4 Ab in the absence or presence of IFN $\alpha$ . Fourteen days later, the percentage of GC-B cells among hlgG4-specific B cells was assessed by flow cytometry (left), and anti-hlgG4 Ab responses (right) were assessed by ELISA on serum. Data from two experiments were pooled. Each dot represents a separate mouse. **(D)** huLangCre-IL-6<sup>fl/fl</sup> mice were generated to target IL-6-deficient (LC<sup>ΔIL-6</sup>) or -sufficient LCs. LCs and keratinocytes (KC) of Cre+ and Cre- mice were sorted, and genomic DNA was extracted for genotyping. Note that the recombined band is only present in Cre+ LCs. **(E)** The serum of *Batf3*<sup>-/-</sup> mice treated with anti-IL-6 or isotype control antibodies was collected, and the concentration of IL-6 was assessed by

Luminex. **(F)** The efficiency of ICOS-L blockade is shown. B cells were stained with anti-ICOS-L. Each dot represents a separate mouse. \*\**p*<0.005, \*\*\**p*<0.001, \*\*\*\**p*<0.0001, ns=not significant.

#### SUPPLEMENTARY FIGURE 3

Validation experiments for CD80/CD86 and other co-stimulatory molecules. **(A)** The role of MHC-II, CD154, CD275, CD80/86, or a combination of these parameters in GC responses was tested *in vitro*. Blocking Abs or isotype control Abs were added to the *in vitro* model simultaneously with T cells. Five days later, the phenotype of T cells (left) and B cells (right) was assessed by flow cytometry. The Tfh and GC B cells in each well were calculated and plotted relative to the average of Tfh and GC B cells in isotype conditions. Data from two independent experiments were pooled. Each dot represents an independent replicate. **(C)** At the end of the *in vitro* cultures with WT and CD80/86 DKO DCs and B cells, the level of CD86 on DCs and **(D)** B cells was determined by flow cytometry, and the MFI values of CD86 were plotted. Data from two independent experiments were pooled.

## References

- Merad M, Sathe P, Helft J, Miller J, Mortha A. The dendritic cell lineage: ontogeny and function of dendritic cells and their subsets in the steady state and the inflamed setting. *Annu Rev Immunol.* (2013) 31:563–604. doi: 10.1146/annurev-immunol-020711-074950
- Yin X, Chen S, Eisenbarth SC. Dendritic cell regulation of T helper cells. *Annu Rev Immunol.* (2021) 39:759–90. doi: 10.1146/annurev-immunol-101819-025146
- Curtsinger JM, Schmidt CS, Mondino A, Lins DC, Kedl RM, Jenkins MK, et al. Inflammatory cytokines provide a third signal for activation of naive CD4+ and CD8+ T cells. *J Immunol.* (1999) 162:3256–62. doi: 10.4049/jimmunol.162.6.3256
- Hilligan KL, Ronchese F. Antigen presentation by dendritic cells and their instruction of CD4+ T helper cell responses. *Cell Mol Immunol.* (2020) 17:587–99. doi: 10.1038/s41423-020-0465-0
- Janeway CA, Medzhitov R. Innate immune recognition. *Annu Rev Immunol.* (2002) 20:197–216. doi: 10.1146/annurev-immunol.20.083001.084359
- Yao C, Zurawski SM, Jarrett ES, Chicoine B, Crabtree J, Peterson EJ, et al. Skin dendritic cells induce follicular helper T cells and protective humoral immune responses. *J Allergy Clin Immunol.* (2015) 136:1387–1397.e7. doi: 10.1016/j.jaci.2015.04.001
- Bouteau A, Kervevan J, Su Q, Zurawski SM, Contreras V, Dereuddre-Bosquet N, et al. DC subsets regulate humoral immune responses by supporting the differentiation of distinct th cells. *Front Immunol.* (2019) 10:1134. doi: 10.3389/fimmu.2019.01134
- Caminschi I, Shortman K. Boosting antibody responses by targeting antigens to dendritic cells. *Trends Immunol.* (2012) 33:71–7. doi: 10.1016/j.it.2011.10.007
- Kato Y, Zaid A, Davey GM, Mueller SN, Nutt SL, Zotos D, et al. Targeting antigen to clec9A primes follicular th cell memory responses capable of robust recall. *J Immunol.* (2015) 195:1006–14. doi: 10.4049/jimmunol.1500767
- Corbett AJ, Caminschi I, McKenzie BS, Brady JL, Wright MD, Mottram PL, et al. Antigen delivery via two molecules on the CD8- dendritic cell subset induces humoral immunity in the absence of conventional “danger. *Eur J Immunol.* (2005) 35:2815–25. doi: 10.1002/eji.200526100
- Li J, Ahmet F, Sullivan LC, Brooks AG, Kent SJ, De Rose R, et al. Antibodies targeting Clec9A promote strong humoral immunity without adjuvant in mice and non-human primates. *Eur J Immunol.* (2015) 45:854–64. doi: 10.1002/eji.201445127
- Lahoud MH, Ahmet F, Kitsoulis S, Wan SS, Vremec D, Lee C-N, et al. Targeting antigen to mouse dendritic cells via Clec9A induces potent CD4 T cell responses biased toward a follicular helper phenotype. *J Immunol.* (2011) 187:842–50. doi: 10.4049/jimmunol.1101176
- Kato Y, Steiner TM, Park H-Y, Hitchcock RO, Zaid A, Hor JL, et al. Display of native antigen on cDC1 that have spatial access to both T and B cells underlies efficient humoral vaccination. *J Immunol.* (2020) 205:1842–56. doi: 10.4049/jimmunol.2000549
- Caminschi I, Proietto AI, Ahmet F, Kitsoulis S, Teh JS, Lo JCY, et al. The dendritic cell subtype-restricted C-type lectin Clec9A is a target for vaccine enhancement. *Blood.* (2008) 112:3264–73. doi: 10.1182/blood-2008-05-155176
- Kervevan J, Bouteau A, Lanza JS, Hammoudi A, Zurawski S, Surenaud M, et al. Targeting human langerin promotes HIV-1 specific humoral immune responses. *PLoS Pathog.* (2021) 17:1–24. doi: 10.1371/journal.ppat.1009749
- Belkaid Y, Harrison OJ. Homeostatic immunity and the microbiota. *Immunity.* (2017) 46:562–76. doi: 10.1016/j.immuni.2017.04.008
- Ginhoux F, Tacke F, Angeli V, Bogunovic M, Loubeau M, Dai X-M, et al. Langerhans cells arise from monocytes *in vivo*. *Nat Immunol.* (2006) 7:265–73. doi: 10.1038/ni1307
- Hoeffel G, Wang Y, Greter M, See P, Teo P, Malleret B, et al. Adult Langerhans cells derive predominantly from embryonic fetal liver monocytes with a minor contribution of yolk sac-derived macrophages. *J Exp Med.* (2012) 209:1167–81. doi: 10.1084/jem.20120340
- Doebel T, Voisin B, Nagao K. Langerhans cells - the macrophage in dendritic cell clothing. *Trends Immunol.* (2017) 38:817–28. doi: 10.1016/j.IT.2017.06.008
- Crotty S. T follicular helper cell differentiation, function, and roles in disease. *Immunity.* (2014) 41:529–42. doi: 10.1016/j.immuni.2014.10.004
- Krishnaswamy JK, Alsén S, Yrlid U, Eisenbarth SC, Williams A. Determination of T follicular helper cell fate by dendritic cells. *Front Immunol.* (2018) 9:2169. doi: 10.3389/fimmu.2018.02169
- Crotty S. T follicular helper cell biology: A decade of discovery and diseases. *Immunity.* (2019) 50:1132–48. doi: 10.1016/j.immuni.2019.04.011
- Kaplan DH. Ontogeny and function of murine epidermal Langerhans cells. *Nat Immunol.* (2017) 18:1068–75. doi: 10.1038/ni.3815
- Bobr A, Olvera-Gomez I, Igyártó BZ, Haley KM, Hogquist KA, Kaplan DH. Acute ablation of Langerhans cells enhances skin immune responses. *J Immunol.* (2010) 185:4724–8. doi: 10.4049/jimmunol.1001802
- Igyártó BZ, Haley K, Ortner D, Bobr A, Gerami-Nejad M, Edelson BT, et al. Skin-resident murine dendritic cell subsets promote distinct and opposing antigen-specific T helper cell responses. *Immunity.* (2011) 35:260–72. doi: 10.1016/j.immuni.2011.06.005
- Durai V, Bagadia P, Granja JM, Satpathy AT, Kulkarni DH, Davidson JT, et al. Cryptic activation of an Irf8 enhancer governs cDC1 fate specification. *Nat Immunol.* (2019) 20:1161–73. doi: 10.1038/s41590-019-0450-x
- Ferris ST, Durai V, Wu R, Theisen DJ, Ward JP, Bern MD, et al. cDC1 prime and are licensed by CD4+ T cells to induce anti-tumour immunity. *Nature.* (2020) 584:624–9. doi: 10.1038/s41586-020-2611-3
- Kaplan DH, Jenison MC, Saeland S, Shlomchik WD, Shlomchik MJ. Epidermal langerhans cell-deficient mice develop enhanced contact hypersensitivity. *Immunity.* (2005) 23:611–20. doi: 10.1016/j.immuni.2005.10.008
- Carotta S, Willis SN, Hasbold J, Inouye M, Pang SHM, Emslie D, et al. The transcription factors IRF8 and PU.1 negatively regulate plasma cell differentiation. *J Exp Med.* (2014) 211:2169–81. doi: 10.1084/jem.20140425
- Wang H, Jain S, Li P, Lin JX, Oh J, Qi C, et al. Transcription factors IRF8 and PU.1 are required for follicular B cell development and BCL6-driven germinal center responses. *Proc Natl Acad Sci U S A.* (2019) 116:9511–20. doi: 10.1073/pnas.1901258116
- Cucak H, Yrlid U, Reizis B, Kalinke U, Johansson-Lindbom B. Type I interferon signaling in dendritic cells stimulates the development of lymph-node-resident T follicular helper cells. *Immunity.* (2009) 31:491–501. doi: 10.1016/j.immuni.2009.07.005
- Sanchis P, Fernández-Gayol O, Comes G, Aguilar K, Escrig A, Giral M, et al. A new mouse model to study restoration of interleukin-6 (IL-6) expression in a Cre-dependent manner: microglial IL-6 regulation of experimental autoimmune encephalomyelitis. *J Neuroinflamm.* (2020) 17:1–17. doi: 10.1186/s12974-020-01969-0
- Kaplan DH, Li MO, Jenison MC, Shlomchik WD, Flavell RA, Shlomchik MJ. Autocrine/paracrine TGF $\beta$ 1 is required for the development of epidermal Langerhans cells. *J Exp Med.* (2007) 204:2545–52. doi: 10.1084/jem.20071401
- Choi YS, Kageyama R, Eto D, Escobar TC, Johnston RJ, Monticelli L, et al. ICOS receptor instructs T follicular helper cell versus effector cell differentiation via induction of the transcriptional repressor Bcl6. *Immunity.* (2011) 34:932–46. doi: 10.1016/j.immuni.2011.03.023



35. Weber JP, Fuhrmann F, Feist RK, Lahmann A, Al Baz MS, Gentz L-J, et al. ICOS maintains the T follicular helper cell phenotype by down-regulating Krüppel-like factor 2. *J Exp Med.* (2015) 212:217–33. doi: 10.1084/jem.20141432
36. Pratama A, Srivastava M, Williams NJ, Papa I, Lee SK, Dinh XT, et al. MicroRNA-146a regulates ICOS-ICOSL signalling to limit accumulation of T follicular helper cells and germinal centres. *Nat Commun.* (2015) 6:6436. doi: 10.1038/ncomms7436
37. Fuentes Marraco SA, Grosjean F, Duval A, Rosa M, Lavanchy C, Ashok D, et al. Novel murine dendritic cell lines: A powerful auxiliary tool for dendritic cell research. *Front Immunol.* (2012) 3:331. doi: 10.3389/fimmu.2012.00331
38. Pigni M, Ashok D, Stevanin M, Acha-Orbea H. Establishment and characterization of a functionally competent type 2 conventional dendritic cell line. *Front Immunol.* (2018) 9:1912. doi: 10.3389/fimmu.2018.01912
39. Watanabe M, Fujihara C, Radtke AJ, Chiang YJ, Bhatia S, Germain RN, et al. Co-stimulatory function in primary germinal center responses: CD40 and B7 are required on distinct antigenpresenting cells. *J Exp Med.* (2017) 214:2795–810. doi: 10.1084/jem.20161955
40. Steiner TM, Heath WR, Caminschi I. The unexpected contribution of conventional type 1 dendritic cells in driving antibody responses. *Eur J Immunol.* (2022) 52:189–96. doi: 10.1002/eji.202149658
41. Satpathy AT, W. KC, Albring JC, Edelson BT, Kretzer NM, Bhattacharya D, et al. Zbtb46 expression distinguishes classical dendritic cells and their committed progenitors from other immune lineages. *J Exp Med.* (2012) 209:1135–52. doi: 10.1084/jem.20120030
42. Schlitzer A, Sivakamasundari V, Chen J, Bin Sumatoh HR, Schreuder J, Lum J, et al. Identification of cDC1- and cDC2-committed DC progenitors reveals early lineage priming at the common DC progenitor stage in the bone marrow. *Nat Immunol.* (2015) 16:718–28. doi: 10.1038/ni.3200
43. Ansaldi E, Farley TK, Belkaid Y. Control of immunity by the microbiota. *Annu Rev Immunol.* (2021) 39:449–79. doi: 10.1146/annurev-immunol-093019-112348
44. Van Panhuys N. TCR signal strength alters T-DC activation and interaction times and directs the outcome of differentiation. *Front Immunol.* (2016) 7:6. doi: 10.3389/fimmu.2016.00006
45. Bhattacharyya ND, Feng CG. Regulation of T helper cell fate by TCR signal strength. *Front Immunol.* (2020) 11:624. doi: 10.3389/fimmu.2020.00624
46. Balkow S, Heinz S, Schmidbauer P, Kolanus W, Holzmann B, Grabbe S, et al. LFA-1 activity state on dendritic cells regulates contact duration with T cells and promotes T-cell priming. *Blood.* (2010) 116:1885–94. doi: 10.1182/blood-2009-05-224428
47. Varga G, Balkow S, Wild MK, Stadtbauer A, Krummen M, Rothoeft T, et al. Active MAC-1 (CD11b/CD18) on DCs inhibits full T-cell activation. *Blood.* (2007) 109:661–9. doi: 10.1182/blood-2005-12-023044
48. Edelson BT, W. KC, Juang R, Kohyama M, Benoit LA, Klekotka PA, et al. Peripheral CD103+ dendritic cells form a unified subset developmentally related to CD8alpha+ conventional dendritic cells. *J Exp Med.* (2010) 207:823–36. doi: 10.1084/jem.20091627
49. Borriello F, Sethna MP, Boyd SD, Schweitzer AN, Tivol EA, Jacoby D, et al. B7–1 and B7–2 have overlapping, critical roles in immunoglobulin class switching and germinal center formation. *Immunity.* (1997) 6:303–13. doi: 10.1016/S1074-7613(00)80333-7
50. Macal M, Jo Y, Dallari S, Chang AY, Dai J, Swaminathan S, et al. Self-renewal and toll-like receptor signaling sustain exhausted plasmacytoid dendritic cells during chronic viral infection. *Immunity.* (2018) 48:730–744.e5. doi: 10.1016/j.immuni.2018.03.020
51. Sage PT, Sharpe AH. *In vitro* assay to sensitively measure T(FR) suppressive capacity and T(FH) stimulation of B cell responses. *Methods Mol Biol.* (2015) 1291:151–60. doi: 10.1007/978-1-4939-2498-1\_13
52. Kolenbrander A, Grewe B, Nemazee D, Überla K, Temchura V. Generation of T follicular helper cells *in vitro*: requirement for B-cell receptor cross-linking and cognate B- and T-cell interaction. *Immunology.* (2018) 153:214–24. doi: 10.1111/imm.12834